

Protecting Sub-Micrometer Surface Features in Polymers from Mechanical Damage Using Hierarchical Patterns

Florian Roessler¹ and Andrés F. Lasagni^{1,2}

¹*Technische Universität Dresden, Institut für Fertigungstechnik, George-Baehr-Str. 3c, 01069 Dresden, Germany
E-mail: florian.roessler@tu-dresden.de*

²*Fraunhofer-Institut für Werkstoff- und Strahltechnik (IWS), Winterbergstraße 28, 01277 Dresden, Germany*

Micro and nano textures on surfaces have shown outstanding properties in several natural examples. Especially, contact properties are in the focus of science including wetting properties, bacteria and cell adhesion of textured surfaces. A critical point of these patterned surfaces is related to the relative low mechanical resistance to scratches, especially when sub-micrometer features are required to provide an enhanced function, such low bacteria adhesion. Therefore, new topographies capable to protect the damage of the sub-micrometer features are necessary. In this work, hierarchical surface patterns are produced on polyimide substrates with the aim of reducing wear of the small scaled features. The hierarchical surface structures are fabricated using Direct laser interference patterning, employing a ns-pulsed Nd:YAG laser, with spatial periods of 0.5 μm and 5 μm . Two and three beam interference setups have been employed, producing surfaces with post-like and hole-like patterns. The wear experiments are performed with 1.5 mm 100Cr6 steel ball oscillating over the surface up to 1000 cycles loaded with 40 mN. The textured surfaces are also characterized using scanning electron microscopy (SEM) and atomic force microscopy (AFM). It was found, that hierarchical patterns consisting on holes with 0.5 μm and 5.0 μm periods can protect the sub-micrometer patterns significantly from mechanical damage and thus prolonging their lifetime.

DOI: 10.2961/jlmn.2018.02.0004

Keywords: laser material processing, microstructure fabrication, direct laser interference patterning, hierarchical surfaces, wear, surface protection

1. Introduction

Surface textures in the range of micrometers and sub micrometers have shown outstanding properties in several natural examples as well as technological applications. Especially, contact properties are in the focus of science and engineering, since the water repellent effect of the lotus leaf has been discovered [1,2]. Less popular but also remarkable is the springtail, which is equipped with a hierarchical pattern and shows an antibacterial and non-wetting behavior. Thus, these animals can live in contact with soil and get not sick [3]. Investigations on bacterial attachment show that surfaces patterned with feature sizes smaller than a bacterium can reduce the bacteria settlement. This range is roughly defined to length scales smaller than 1 μm . For example, periodic patterned surfaces in SU-8 or PI with spatial periods of 0.5 μm have shown to be capable to reduce bacteria adhesion to less than 50 % [4–7].

In the past, the stability and wear of micro patterns has been also investigated. The focus has been set on wear and friction reduction on metallic or coated surfaces under lubricated or dry conditions [8–12]. It was found, that micro textured surfaces can reduce friction and wear, since wear particles sink into the fabricated cavities and are kept away from the contact area. Indeed, contact properties must be provided under everyday conditions such as touching, scratching or other mechanical impacts.

A large number of fabrication techniques have been developed to fabricate micro and nano patterned surfaces. Molding or imprinting methods have been used frequently to equip surfaces patterns in a repetitive fabrication process, but these processes require stamps and molds, which have to

be fabricated with other methods [13–19]. Photolithography and etching processes can be used to obtain the complex structures [14,17–20]. Typically, this multi-step processes are associated with long fabrication durations, many processing chemicals and clean-room conditions. In consequence, the processing costs are expensive, especially if large areas or high number of parts have to be treated.

More efficient and flexible fabrication methods are laser based ablative processes. Especially, Direct Laser Interference Patterning (DLIP) is a well-established method capable to fabricate periodic structures in the range of micro- and sub-micrometer (e.g. 0.18 μm to 30 μm spatial period) in several materials including metals, polymers and ceramics [21–31]. The main advantages of this technology is that materials can be treated without the need of using clean room conditions (like in optical lithography) as well as without masks or chemicals. Thus, the fabrication is cost-efficient and flexible at the same time.

Concerning the fabrication of hierarchical surface patterns, a combination of direct laser writing (DLW) for large feature sizes and DLIP for small pattern sizes was applied to fabricate two-level hierarchical patterns on polyimide [32]. Using only the DLIP method, also three-level hierarchical patterns were fabricated in PET using a two-step process [33]. Also on metals (titanium, stainless steel), two-level hierarchical patterns with different spatial periods were achieved employing DLIP [34,35]. Hierarchical patterns were also produced utilizing the self-organizing laser induced period surface structures (LIPSS) by combining sub-micrometer LIPSS with larger (couple of

micrometer) pattern geometries obtained with DLW or DLIP [36–39].

In this work, direct laser interference patterning is used to fabricate multiple-scale surface structures on polyimide. The main objective is to develop multiple-scaled surface textures in order to protect sub-micrometer features showing an antibacterial behavior from wear and mechanical degradation. Two and three-beam interference configurations are used to produce post-like and hole-like patterns with feature sizes between $0.5\ \mu\text{m}$ and $5\ \mu\text{m}$, using a nanosecond pulsed Nd:YAG laser on its third harmonic wavelength of $355\ \text{nm}$. The $0.5\ \mu\text{m}$ period was selected, since the bacteria adhesion for this spatial period could be strongly reduced in the past. Wear experiments are performed with a 100Cr6 steel ball. The textured surfaces are also characterized using scanning electron microscopy (SEM) and atomic force microscopy (AFM).

2. Experimental

For the hierarchical DLIP structuring process, Polyimide foils (PI, Kapton 200 HN purchased from Pütz Folien, Germany) with a thickness of $50\ \mu\text{m}$ were used as received. A nanosecond pulsed Nd:YAG laser (Quanta Ray 290 Pro, Spectra Physics) provided a wavelength of $355\ \text{nm}$ as the third harmonic of the $1064\ \text{nm}$ fundamental wavelength. The pulse duration was $8\ \text{ns}$ and the repetition rate was $10\ \text{Hz}$. Hole-like and post-like structures were fabricated using a beam-splitter configuration with three and two laser beams, respectively, as shown in Fig. 1. A detailed description of the experimental setup has been already published elsewhere [40]. Spatial periods of $0.5\ \mu\text{m}$ and $5.0\ \mu\text{m}$ were obtained using overlapping angles of $\theta = 41.6^\circ$ and 4.1° , respectively with the two-beam configuration, which is shown in Fig. 1a. The resulting line-like intensity distribution is shown in Fig. 1b. For three-beam interference, shown in Fig. 1d, the angle of incidence of each individual beam was set to $\theta = 24.2^\circ$ and 2.4° , obtaining 0.5 and $5\ \mu\text{m}$ spatial periods, respectively. The obtained two-dimensional dot-like intensity distribution is shown in Fig. 1e. The laser fluence was varied between $0.35\ \text{J}/\text{cm}^2$ and $1.0\ \text{J}/\text{cm}^2$. In all cases, the laser beams were not focused on the sample and

the patterned area per pulse varied between $0.024\ \text{cm}^2$ and $0.14\ \text{cm}^2$.

The wear behavior of single scale and hierarchical patterns on PI was characterized using a nanotribometer (CSM instruments) in ball on disk configuration.

The 100Cr6 steel balls ($1.5\ \text{mm}$ in diameter) were cleaned with isopropanol and were rotated before each experiment, that the area in contact with the PI surface was unaffected from the previous experiment. In all cases, the applied normal load was $40\ \text{mN}$. During the measurement, the substrate oscillates linearly on a distance of $1\ \text{mm}$ with a maximum speed of $5\ \text{mm}/\text{s}$. The forces and the moving distance were controlled with fiber optical distance sensors. The ball holder was located at a cantilever with a known spring constant, which allows calculating the forces from the deflection. After 1000 cycles the substrate was removed and the wear track was analyzed using confocal microscopy (Sensofar S neox). For structures with a spatial period of $5\ \mu\text{m}$, a $150\times$ objective with a lateral resolution of $140\ \text{nm}$ and a vertical resolution $\sim 2\ \text{nm}$ was used [41,42]. Structures with smaller spatial periods were measured with an atomic force microscope (nanosurf coreAFM). In the last case, the lateral scan-range was set to $20\ \mu\text{m} \times 20\ \mu\text{m}$ and the vertical range was $12\ \mu\text{m}$. The low noise of the measurement ($0.25\ \text{nm}$) allows to characterize small periods (e.g. $0.5\ \mu\text{m}$). The measurements were performed in a dynamic measuring or amplitude mode (AM-AFM), where the cantilever oscillates on a high frequency in a certain distance close to the surface.

High resolution images were obtained from scanning electron microscopy (SEM) using a XL30 ESEM (from Philips) in secondary electron mode at 10 to $15\ \text{kV}$ operation voltage. Prior observations, the samples were coated with a $2\ \text{nm}$ layer of Au/Co alloy.

3. Results and discussion

Direct laser interference patterning with two-beam and three-beam configuration was used to create post-like and hole-like patterns on the surface of PI substrates, respectively. Post-like structures were produced in two steps, consisting on producing the line-like patterns with the two-

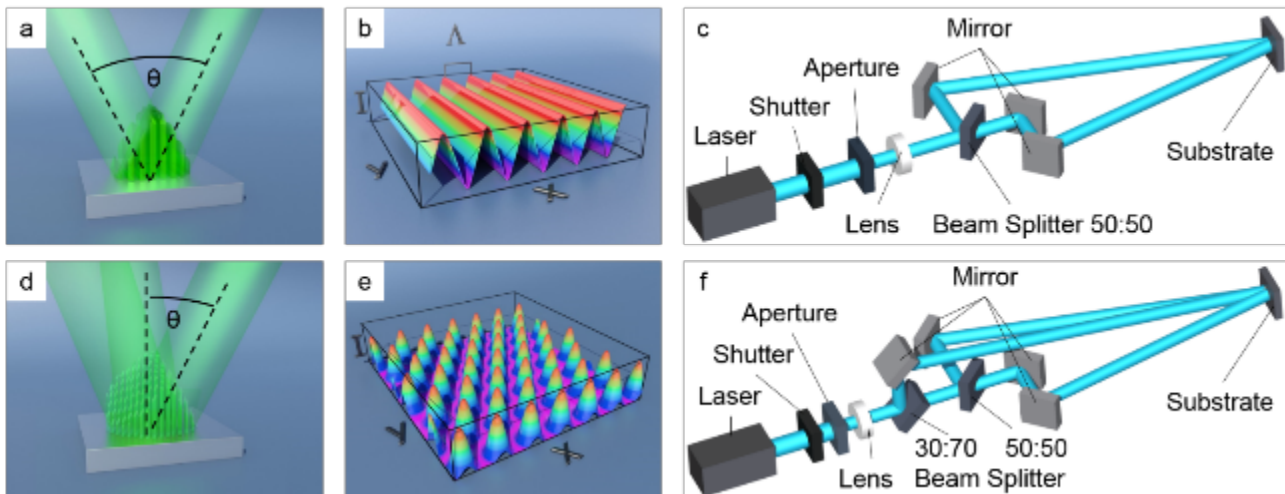


Fig. 1. (a) Two interfering laser beams over the materials' surface producing (b) a line-like periodic intensity distribution. (c) Beam splitter configuration for two-beam setup to fabricate line-like surface patterns. (d) Scheme of three interfering laser beams producing (e) a dot-like periodic intensity distribution. (f) Three-beam configuration to fabricate hole-like surface patterns.

beam configuration (Fig. 1c), rotating the substrate 90° and irradiating the sample again with the same configuration. The hole-like patterns were produced in a single irradiation step with the three-beam interference setup (Fig. 1f).

Fig. 2 shows SEM images of structures fabricated using this structuring strategy. For example, post-like structures with $\Lambda = 5 \mu\text{m}$ were produced using a laser fluence $F = 1.0 \text{ J/cm}^2$ (Fig. 2a). In the case of shorter spatial periods, (e.g. $\Lambda = 0.5 \mu\text{m}$, Fig. 2b) the laser fluence had to be reduced to $F = 0.35 \text{ J/cm}^2$ in order to produce patterns with a better homogeneity. A similar behavior was observed for the hole-like patterns fabricated with three interfering laser beams ($F = 0.75 \text{ J/cm}^2$ for $\Lambda = 5 \mu\text{m}$, see Fig. 2c and $F = 0.35 \text{ J/cm}^2$ for $\Lambda = 0.5 \mu\text{m}$).

The topology of the fabricated patterns results from the local ablation that is produced at the interference maxima positions. This behavior can be explained by the nature of the interaction of the UV laser light with the PI substrate. As reported before, due to the short wavelength used (355 nm), the laser-photon energy is mainly transferred to the material resulting in a photo-chemical process [43,44]. Thereby, the material is ablated due to bond-breaking in the polymer molecules. In addition, high pressure provoked by the ablation products occurs during the laser pulse. Thus, the fragments are pushed out of ablated areas (some of this particles can be recognized especially in Fig. 2a, b and c). In the area of the interference minima, where the laser fluence is smaller than the threshold fluence required for ablation, almost no surface modification is visible for the larger periods (5 μm). This behavior is reflected by the sharp edge at the top of the structure morphology, which is notably shown in Fig. 2a, c. Only a very small amount of molten material can be observed, surrounding the ablated areas. On the surfaces treated with the shorter spatial period of 0.5 μm

(see Fig. 2b and d), the non-ablated area is completely covered with a layer of resolidified melt, since the lateral extension of this plateau is smaller conditioned by the smaller period.

In addition to the surface morphology analyses, also other topographical parameters (the structure depth, spatial period) of the fabricated patterns was determined. From the topography obtained with AFM and confocal microscopy, the structure depth is defined as the maximal difference in z-direction between the position of the lowest points and the highest points within one periodic structure and the average value is calculated from at least 10 measured structure depth per pattern.

The highest structure depth was measured for the 5 μm patterns. For example, the depth of the post-like patterns was $1.57 \pm 0.12 \mu\text{m}$ at a fluence of $F = 1.0 \text{ J/cm}^2$. For the hole-like structure, the structure depth was $1.03 \pm 0.10 \mu\text{m}$ at $F = 0.75 \text{ J/cm}^2$. The post-like patterns with 0.5 μm spatial period fabricated with 0.35 J/cm^2 presented a structure depth of $0.21 \pm 0.06 \mu\text{m}$, while the hole-like structures have a depth of $0.14 \pm 0.03 \mu\text{m}$. A general observation that arises when comparing both patterns, is that the depth of the post-like pattern is larger (66 %) than for the hole-like structure, wheatear the nominal fluence is the same. The reason for this behavior is given by the fact, that two laser pulses (with line-like intensity distribution) are needed to produce the post-like patterns, which means that the areas where two pulses overlap are irradiated twice. Thus, the cumulated fluence of two line-like irradiations at the position of the maximum in both directions is 4.0 J/cm^2 (with $F = 1.0 \text{ J/cm}^2$ nominal fluence, which means that the fluence at the interference maxima is 2.0 J/cm^2). In comparison, for the three-beam configuration, the cumulated fluence at the interference maxima is 2.25 J/cm^2 , resulting from adding three times the

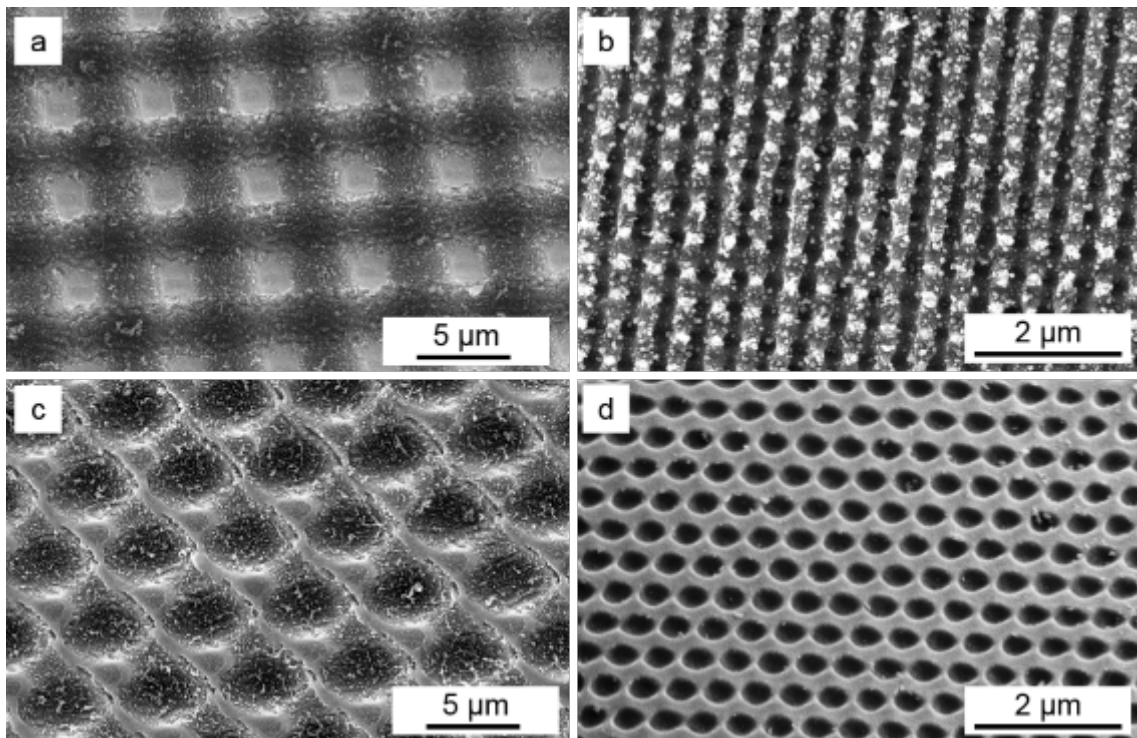


Fig. 2. SEM images of post-like structures with (a) $\Lambda = 5 \mu\text{m}$ ($F = 1.0 \text{ J/cm}^2$), (b) $\Lambda = 0.5 \mu\text{m}$ ($F = 0.35 \text{ J/cm}^2$) spatial period fabricated with two-beam interference setup and hole-like structures (c) $\Lambda = 5 \mu\text{m}$ ($F = 0.75 \text{ J/cm}^2$), (d) $\Lambda = 0.5 \mu\text{m}$ ($F = 0.35 \text{ J/cm}^2$) spatial period fabricated with three-beam interference configuration.

nominal fluence of 0.75 mJ/cm^2 (which is 56 % lower than the previous case).

To fabricate the two-level hierarchical micro-patterns, firstly, the periodic structure with the largest length scale (e.g. $5 \mu\text{m}$) was fabricated. After that, the angle between the beams was increased and the previously treated area is consecutively re-irradiated creating the sub-micrometer structure over the previous one.

The analysis of the structure depth was also in this case conducted with AFM. Pseudo-color and 3D images of the topography are shown in Fig. 4. Exemplarily, $0.5 \mu\text{m}$ post-like pattern on $5 \mu\text{m}$ hole-like structure is shown in Fig. 4a, b and $0.5 \mu\text{m}$ hole-like pattern on $5 \mu\text{m}$ post-like pattern in Fig. 4c, d. As it can be seen in the AFM images, the $5 \mu\text{m}$ periodic structures are predominant since larger structure depth are possible for the large periods, compared to the

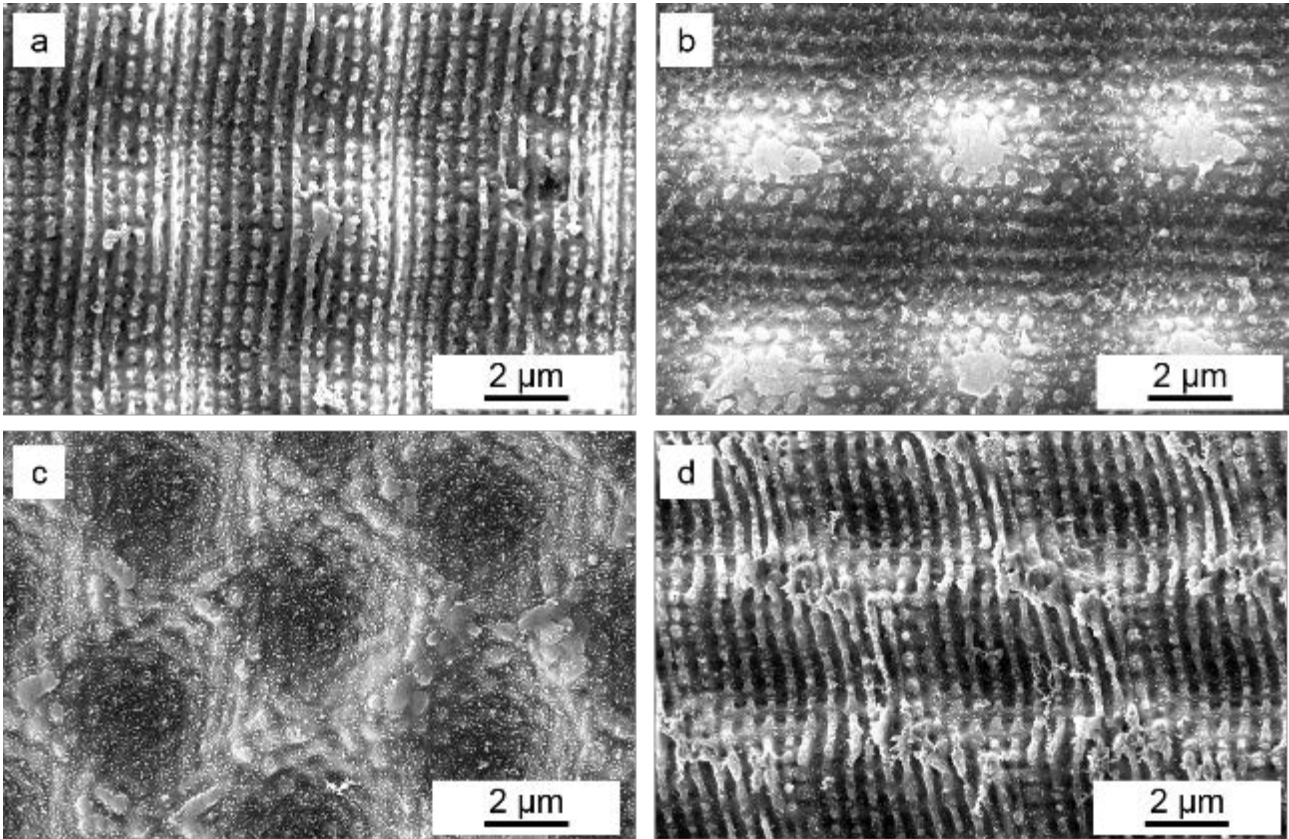


Fig. 3. SEM images of hierarchical patterned PI substrates with sub-micrometer patterns of $\Lambda = 0.5 \mu\text{m}$ on top of large patterns with $\Lambda = 5 \mu\text{m}$. (a) small posts on large posts fabricated with 0.35 J/cm^2 and 1.0 J/cm^2 , respectively. (b) Small holes on large post-like pattern fabricated with 0.35 J/cm^2 and 1.0 J/cm^2 , respectively. (c) small hole-like on large hole-like pattern fabricated with 0.35 J/cm^2 and 0.75 J/cm^2 , respectively and (d) small posts on large hole-like structure fabricated with 0.35 J/cm^2 and 1.0 J/cm^2 , respectively.

Considering that the treated area per spot (and per laser pulse) was relatively large (up to 0.14 cm^2) no significant fluctuations in the surface topography were observed. Examples of the produced hierarchical patterns are shown in Fig. 3. In all cases, a two-level hierarchy was obtained consisting of (i) the $5 \mu\text{m}$ patterns (1st level) and (ii) the $0.5 \mu\text{m}$ patterns (2nd level). Four combinations of small and large scale post-like and hole-like patterns can be found. The first patterns consist of $\Lambda = 5 \mu\text{m}$ post-like pattern fabricated with an energy density of $F = 1.0 \text{ J/cm}^2$ overlaid by smaller post-like structures with $\Lambda = 0.5 \mu\text{m}$ (Fig. 3a) or by a $\Lambda = 0.5 \mu\text{m}$ hole-like structure (Fig. 3b) fabricated with $F = 0.35 \text{ J/cm}^2$ each. Additionally, patterns with $\Lambda = 5 \mu\text{m}$ hole-like patterns fabricated with an energy density of $F = 0.75 \text{ J/cm}^2$ were overlaid by smaller hole-like structures with $\Lambda = 0.5 \mu\text{m}$ (Fig. 3c) or by a $\Lambda = 0.5 \mu\text{m}$ post-like structure (Fig. 3d) fabricated with $F = 0.35 \text{ J/cm}^2$, each. In all cases, the small scale structure totally covers the first surface pattern.

smaller features. This can be explained since the achievable structure depth for the large periods are 5.2 times the structure depth of the smaller features according to the analyses from the previous section (Fig. 2). For example, in the case of the small posts on large holes shown in Fig. 4a, the holes are 4.9 times deeper. In the case of the small holes on large posts shown in Fig. 4c, the posts are 11.2 times higher than the holes.

The total structure depth of all hierarchical patterns are shown in Table 1. These achieved values are in accordance to the sum of the structure depths obtained in the single scale patterns (e.g. average depth of hierarchical holes on holes is $1.13 \mu\text{m}$, is similar to $1.03 \mu\text{m}$ of the $5 \mu\text{m}$ holes plus $0.14 \mu\text{m}$ of the $0.5 \mu\text{m}$ holes, summed $1.17 \mu\text{m}$).

The structures with the hole-like pattern shown very similar values to the summed depth of the single scale patterns in the average value and in the range of the error. The structures with the post-like patterns on top have noticeable differences in the average values, but respecting the tolerances, the values are still in accordance.

Table 1: Structure depth of the hierarchical patterns compared to the summed depth of the corresponding single scale patterns

5 μm pattern	0.5 μm pattern	Hierarchical structure depth	Summed depth of single scale patterns	Difference [%]
post-like	post-like	$(1.53 \pm 0.08) \mu\text{m}$	$(1.78 \pm 0.18) \mu\text{m}$	- 14
post-like	hole-like	$(1.71 \pm 0.05) \mu\text{m}$	$(1.71 \pm 0.15) \mu\text{m}$	0
hole-like	post-like	$(1.03 \pm 0.17) \mu\text{m}$	$(1.24 \pm 0.16) \mu\text{m}$	- 17
hole-like	hole-like	$(1.13 \pm 0.10) \mu\text{m}$	$(1.17 \pm 0.13) \mu\text{m}$	- 5

Finally, the fabricated surface patterns as well as a non-treated surface (reference) were used for the wear experiments in a ball on disk configuration.

In a first set of experiments, the depth of the wear track was analyzed using confocal microscopy. Since the cross section of the wear track is formed by a circular segment which is related to the spherical shape of the counterpart, the maximum depth of the wear track was used to compare the different surface conditions. The measured values were all normalized to the value of the reference surface and are shown in Fig. 5. The depth of the wear track of the reference PI surface was $0.17 \pm 0.01 \mu\text{m}$.

As it can be seen in Fig. 5, the deepest wear track was found on the 5 μm post-like pattern, where the normalized

measured wear was 3.58 ± 0.38 . This means, that during the same load cycle a 3.5 times deeper wear track was observed. The absolute value of the wear depth is $(0.62 \pm 0.07) \mu\text{m}$, which corresponds to 36 % of the structure depth. The 5 μm hole-like pattern shows a normalized value of 2.19 ± 0.30 , which is roughly the double of the wear on the reference PI surface. In the case of the 0.5 μm structures, a value of ~ 2.2 was measured for the post-like pattern and ~ 1.1 for the hole-like pattern. This means that the post-like pattern show a stronger wear than the hole-like structures. This can be explained due to the more stable topography of the holes compared to the weak posts, since the material in the hole-like pattern is laterally linked (comparable to a honeycomb), while the posts are stand-alone features. Thus, during the

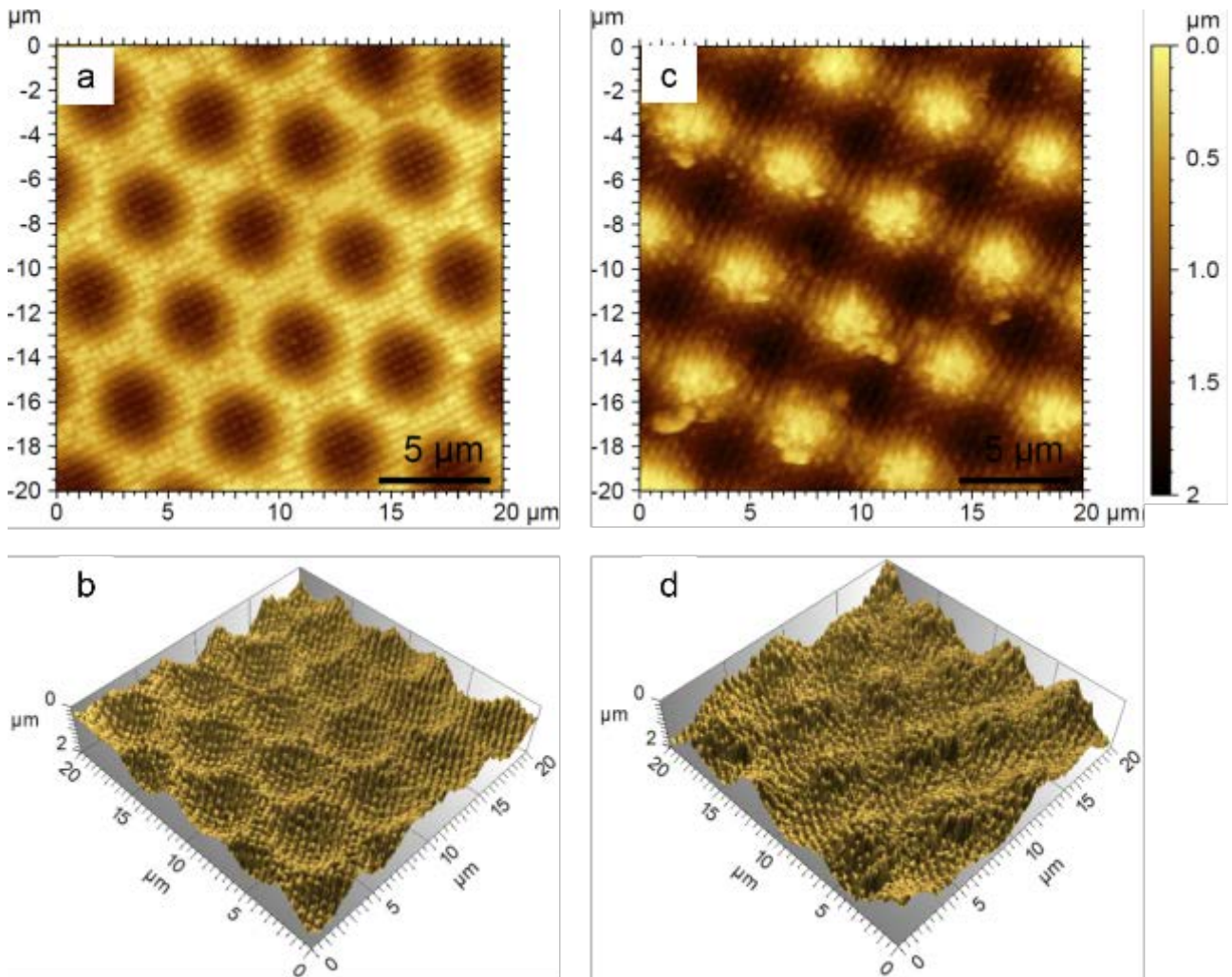


Fig. 4. (a) Surface topography in pseudo colors and (b) three dimensional surface of a hierarchical pattern with 0.5 μm post-like structure on 5 μm hole-like structure obtained from AFM. (c) Surface topography and (d) three dimensional surface of a 0.5 μm hole-like pattern on a 5 μm post-like pattern.

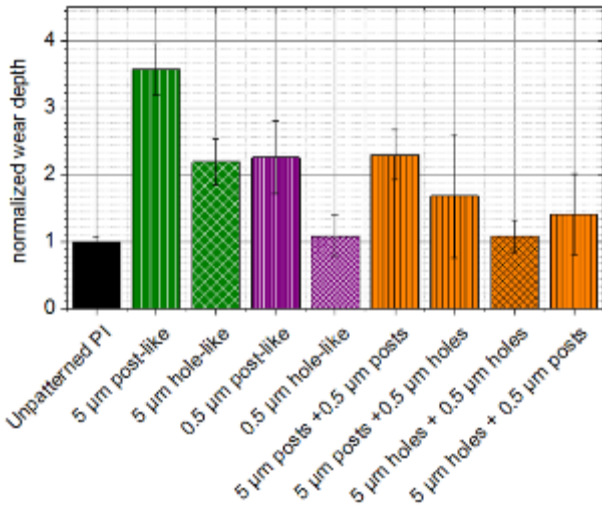


Fig. 5. Normalized wear depth after 1000 cycles, linear oscillation using a 1.5 mm steel ball and a normal load of 40 mN corresponding to the unpatterned PI substrate ($1 \rightarrow 0.17 \mu\text{m}$)

mechanical load, the stress can be distributed in the hole-like pattern as in a network between the features. However, it has to be mentioned that the wear track on both 0.5 μm structures is deeper than the structure depth, which means the complete structure was destroyed in the area of the wear track. Furthermore, the results of the single scale structures show that structures of 0.5 μm get easily damaged which can be explained by the small structure height.

The results for the hierarchical patterns, show in general lower wear depth compared to the large scale patterns. For hierarchical patterns consisting of the 5 μm post-like pattern with 0.5 μm post-like and hole-like pattern on top, relative wear values of 2.29 ± 0.37 and 1.68 ± 0.92 were measured, respectively (Fig. 5). Thus, the small scale pattern seems to reduce the wear, while holes reduce it in average stronger than posts, which again can be explained by the more stable topography of the holes.

A similar effect was observed on the hierarchical patterns based on 5 μm hole-like pattern. The normalized wear depth for the pattern with 0.5 μm holes and posts on

top was 1.08 ± 0.25 and 1.41 ± 0.61 , respectively. This means that especially for the hierarchical pattern with 5 μm and 0.5 μm holes, the measured wear was only 8% higher than the reference. This behavior is unclear and further investigations are required. Also, the influence of the normal load, the speed and the number of cycles on the wear depth cannot be determined from these experiments. Furthermore, several studies have shown that the UV laser treatment of PI causes chemical changes of the material due to bond breaking [43-47]. The affected depth has been reported to be between 0.5 and 60 nm [43,44,48]. Therefore, these chemical changes could also have an influence on the stability of the material and thus also explain why the patterned surfaces show in general more wear than the non-irradiated PI material. Nevertheless, both the wear track depth and the depth of the produced structures is much larger than the depth of the chemical modified material and thus, also the surface morphology might affect the wear behavior.

In addition to the quantitative characterization of wear behavior, SEM images of the wear tracks are of relevant importance for determining if a combination of surface topographies can be capable to protect the smaller features which is necessary to prolong their lifetime and thus the surface functions (e.g. antibacterial performance). These images are shown in Fig. 6, for single scale and hierarchical surface patterns.

In Fig. 6a, the wear track of the 0.5 μm post-like pattern is shown. It is visible that the surface pattern is completely destroyed (as reported before, the depth of the wear track was larger than the structure depth of the post). Fig. 6b shows the wear track of the 0.5 μm hole-like pattern. The image corresponds to the transition from the wear track to non-affected areas. Thus, the pattern is visible in the upper part, while the structure was totally destroyed at the positions where the steel ball was in contact with the polymer surface (lower part). The behavior is different for the larger single-scale patterns. For example, from Fig. 6c, it can be seen that the single scale 5 μm post-like patterns are only partially damaged after the wear experiments. The tops of the posts are flattened compared to the untreated posts

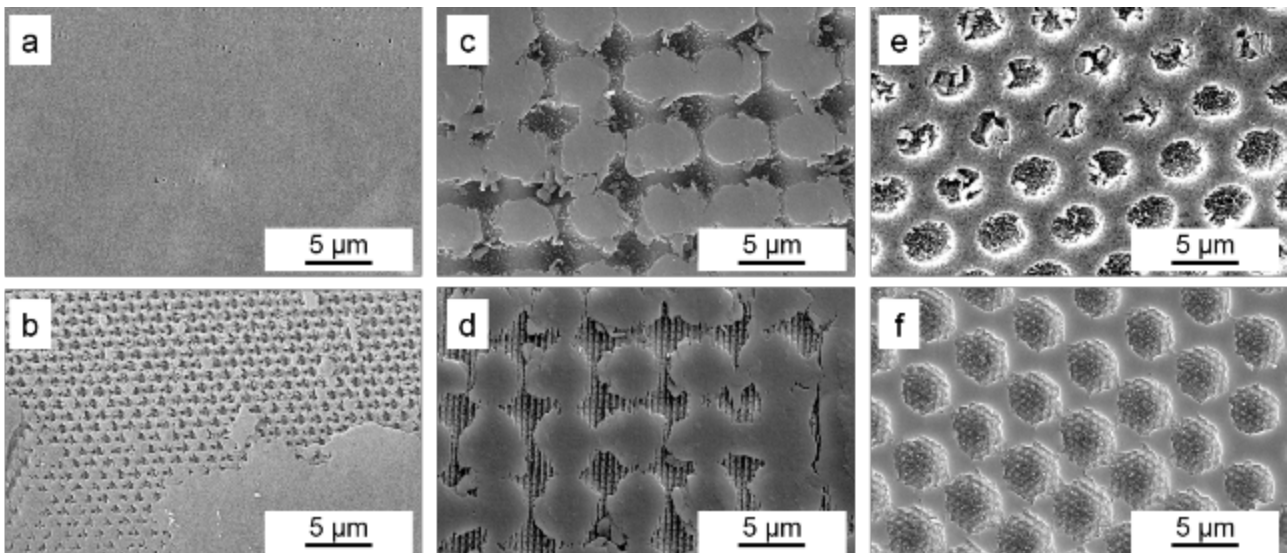


Fig. 6. SEM images of the wear tracks on patterned surfaces after 1000 cycles of linear oscillation of a 1.5 mm steel ball over the substrate with a normal load of 40 mN. Surface patterns: (a) 0.5 μm post-like, (b) 0.5 μm hole-like, (c) 5 μm post-like, (d) hierarchical 0.5 μm post-like on 5 μm post-like, (e) 5 μm hole-like and (f) hierarchical 0.5 μm hole-like on 5 μm hole-like.

(Fig. 2a). It is also visible, that material was reshaped in a lateral direction. Also, a part of the material removed from the tops formed ridges between the single posts in parallel and perpendicular to the movement direction (left to right). A similar effect can be seen in Fig. 6d, where a hierarchical pattern with small posts on large posts is shown after the wear experiments. The tops of the large posts are flattened and ridges were formed between the large posts. Additionally, the small scale structure is completely destroyed in the areas of direct contact between steel ball and PI substrate. However, at the bottom of the large scale posts, the 0.5 μm post-like structure is well-visible and has not been affected.

In Fig. 6e, a single scale 5 μm hole-like pattern is shown. The difference to untreated material is not as clear as on the post-like structure. Two particular characteristics are visible: (i) smaller holes, which indicate a partial damage of the surface (and thus removal of material since the hole-diameter decrease with the depth) and (ii) wear particles within the remaining holes. From the literature it is known, that this is a typical behavior for tribological systems showing a reduction of the friction and wear (for example on micro patterned surfaces on steel or titanium [8–12]). This effect has been explained by the fact that wear particles arising during friction conditions are stored in the cavities and thus they are kept away from the contact zone.

Fig. 6f shows the hierarchical pattern with large and small scale hole-like pattern after the wear experiments. Here, the hole's diameter is also smaller than on the initial surface (Fig. 2c). Furthermore, the top of the surface has been flattened and the small-scale 0.5 μm holes have been completely destroyed at the contact zone. Nevertheless, similarly to the hierarchical post patterns (Fig. 6d), the small scale pattern within the 5.0 μm holes remained undamaged. In consequence, the hierarchical pattern can be used to protect a small scale pattern from wear or mechanical damage. This result is of great importance when preventing damage of sub-micrometer features providing surfaces with enhanced functions, such antibacterial performance [4,5,7].

Preliminary experiments recently conducted, have satisfactory shown that the produced hierarchical patterns also reduced the adherence of bacteria. However, additional test are required to statically validate these results and will be publish in the future.

4. Conclusions

Direct laser interference patterning has been used to fabricate both single-scale and hierarchical surface patterns on polyimide substrates. Post-like and hole-like structures with spatial periods of 0.5 μm and 5 μm were fabricated using two and three-beam interference patterning configurations, respectively. The hierarchical patterns were produced by fabricating first the large scale pattern (5.0 μm) and then the smaller one (0.5 μm).

Concerning the wear behavior of the laser treated surfaces, it has been shown that hole-like patterns present less wear than post-like patterns what can be explained due to the more stable topography of the holes (like a honeycomb) compared to the weak posts. In addition, patterns with larger periods (5.0 μm) and deeper surface structures showed also a higher wear resistance compared to the smaller patterns (0.5 μm).

In the case of the hierarchical patterns, it could be successfully demonstrated that the larger surface patterns (especially with the hole-like geometry) can be used to reduce damage of the sub-micrometer features and thus prolonging their life time. This property is elemental to assure certain surface functions (requiring sub-micrometer features), such antibacterial properties.

Acknowledgements

This work was supported by the Reinhart-Koselleck Grant of the German Research Foundation (Deutsche Forschungsgemeinschaft, DFG) under Project LA 2513/7-1 and under DFG project "Mechanically stable anti-adhesive polymer surfaces" (LA-2513 4-1).

References

- [1] K. Koch, B. Bhushan and W. Barthlott: *Soft Matter*, 4, (2008) 1943.
- [2] W. Barthlott and C. Neinhuis: *Planta* 202, (1997) 1–8.
- [3] R. Helbig, J. Nickerl, C. Neinhuis and C. Werner: *PloS one* 6, (2011) e25105.
- [4] A. J. Scardino, E. Harvey and R. de Nys: *Biofouling* 22, (2006) 55–60.
- [5] R. Helbig, D. Günther, J. Friedrichs, F. Rößler, A. Lasagni and C. Werner: *Biomater. Sci.* 4, (2016) 1074.
- [6] D. Günther, D. Scharnweber, R. Hess, C. Wolf-Brandstetter, M. große Holthaus, A. F. Lasagni: "High precision patterning of biomaterials using the direct laser interference patterning technology" in "Laser Surface Modification of Biomaterials", ed by. R. Vilar, (Woodhead Publishing, 2016) ch.1, p.3.
- [7] L.-C. Xu and C. A. Siedlecki: *Acta biomater* 8, (2012) 72.
- [8] J. Bonse, R. Koter, M. Hartelt, D. Spaltmann, S. Pentzien, S. Höhm, A. Rosenfeld and J. Krüger: *Appl. Phys. A* 117, (2014) 103.
- [9] I. Etsion: *J. Tribol.* 127, (2005) 248.
- [10] C. Gachot, A. Rosenkranz, L. Reinert, E. Ramos-Moore, N. Souza, M. H. Müser and F. Mücklich: *Tribol Lett* 49, (2013) 193.
- [11] K. Jones and S. R. Schmid: *Procedia Manuf.* 5, (2016) 568.
- [12] Z. Wang, Q. Zhao and C. Wang: *Micromachines* 6, (2015) 1606.
- [13] J.-T. Chen, D. Chen and T. P. Russell: *ACS J. Surfaces Colloids* 25, (2009) 4331.
- [14] D. Copic, S. J. Park, S. Tawfick, De Volder, Michael F L and A. J. Hart: *Lab Chip* 11, (2011) 1831.
- [15] S. Dai, D. Zhang, Q. Shi, X. Han, S. Wang and Z. Du: *CrystEngComm* 15, (2013) 5417.
- [16] W. Ge and C. Lu: *Soft Matter* 7, (2011) 2790.
- [17] Y. Lee, W. Lee and J.-K. Lee: *Thin Solid Films* 516, (2008) 3431.
- [18] Y. Lee, S.-H. Park, K.-B. Kim and J.-K. Lee: *Adv. Mater.* 19, (2007) 2330.
- [19] G. Shi, N. Lu, H. Xu, Y. Wang, S. Shi, H. Li, Y. Li and L. Chi: *J. Colloid Interface Sci.* 368, (2012) 655.

- [20]F. Dawan, N. Morampudi, Y. Jin and E. Woldesenbet: *Microelectron. Eng.* 114, (2014) 105.
- [21]F. Beinhorn, J. Ihlemann, P. Simon, G. Marowsky, B. Maisenhölder, J. Edlinger, D. Neuschäfer and D. Anselmetti: *Appl. Surf. Sci.* 138-139, (1999) 107.
- [22]M. Garliauskas, E. Stankevičius and G. Račiukaitis: *Opt. Mater. Express* 7, (2017) 179.
- [23]J. Huang, S. Beckemper, A. Gillner and K. Wang: *J. Micromech. Microeng.* 20, (2010) 95004.
- [24]J.-H. Klein-Wiele and P. Simon: *Appl. Phys. Lett.* 83, (2003) 4707.
- [25]S. Riedel, M. Schmotz, P. Leiderer and J. Boneberg: *Appl. Phys. A*, 101 (2010) 309.
- [26]E. Roitero, F. Lasserre, M. Anglada, F. Mücklich and E. Jiménez-Piqué: *Dent. Mater. J.* 33, (2017) e28.
- [27]A. Rosenkranz, C. Gachot, E. Ramos-Moore and F. Mücklich: *Tribology Online* 11, (2016) 575.
- [28]F. Rößler, T. Kunze and A. F. Lasagni: *Opt. Express* 25, (2017) 22959.
- [29]P. Simon and J. Ihlemann: *Appl. Surf. Sci.* 109, (1997) 25.
- [30]E. Stankevičius, M. Gedvilas, B. Voisiat, M. Malinauskas and G. Račiukaitis: *Lith. J. Phys.* 53, (2013) 227.
- [31]T. Roch, E. Beyer and A. Lasagni: *Diamond Relat. Mater.* 19, (2010) 1472.
- [32]M. Steger: *JLMN* 8, (2013) 210.
- [33]F. Rößler, D. Günther and A. F. Lasagni: *Adv. Eng. Mater.* 18, (2016) 1755.
- [34]M. Bieda, E. Beyer and A. F. Lasagni: *J. Eng. Mater. Technol.* 132, (2010) 31015.
- [35]T. Roch, M. Bieda, A. Lasagni: *Laser Magazin*, (2010) 30.
- [36]A. Lasagni, A. Manzoni and F. Mücklich: *Adv. Eng. Mater.* 9, (2007) 872.
- [37]A. F. Lasagni, P. Shao, J. L. Hendricks, C. M. Shaw, D. C. Martin and S. Das: *Appl. Surf. Sci.* 256, (2010) 1708.
- [38]M. Martínez-Calderon, A. Rodríguez, A. Dias-Ponte, M. C. Morant-Miñana, M. Gómez-Aranzadi and S. M. Olaizola: *Appl. Surf. Sci.* (2015).
- [39]M. V. Rukosuyev, J. Lee, S. J. Cho, G. Lim and M. B. Jun: *Appl. Surf. Sci.* 313, (2014) 411.
- [40]A. Lasagni, C. Holzapfel and F. Mücklich: *Appl. Surf. Sci.* 253, (2006) 1555.
- [41]Leica Microsystems Ltd., “Leica DCM 3D. Dual Core 3D Profiler combines Confocal Imaging and Interferometry”, 2010.
- [42]S. Sensofar-Tech, “S neox. 3D Optical Profiler. Objectives Specification”.
- [43]R. Srinivasan: *Appl. Phys. A* 56, (1993) 417.
- [44]R. Srinivasan and B. Braren: *Chem. Rev.* 89, (1989) 1303.
- [45]A. Brezini: *Phys. Stat. Sol. A* 127, (1991) K9
- [46]Q. Lu, M. Li, Z. Zhu, Z. Wang: *J. Appl. Polym. Sci.* 82, (2001) 2739.
- [47]R. Srinivasan, B. Braren, R. W. Dreyfus: *Appl. Phys.* 61, (1987) 372.
- [48]Z. Qin, T. He, Y. Zhang: *Appl. Phys. A* 66, (1998) 441.

(Received: May 14, 2018, Accepted: August 26, 2018)